Reduced constant-cost implementations of Clifford operations using global interactions

Jonathan Nemirovsky, Lee Peleg, Amit Ben Kish, and Yotam Shapira*

Quantum Art, Ness Ziona 7403682, Israel

We investigate quantum circuits built from arbitrary single-qubit operations combined with programmable all-to-all multiqubit entangling gates that are native to, among other systems, trappedion quantum computing platforms. We report a constant-cost of no more than 6 application of such Clifford entangling multiqubit gates to realize any sequence of Clifford operations of any length, without ancillae. Furthermore, we show that any sequence of CNOT gates of any length, can be replaced with 5 applications of such Clifford entangling multiqubit gates, without ancillae. We investigate the required qubit drive power that is associated with these implementations. Our work introduces a practical and computationally efficient algorithm to realize these compilations.

Clifford operations are central to many quantum information processing applications such as quantum error correction, simulation algorithms [1], generation of pseudo-random unitaries [2–4], compilation of quantum circuits and benchmarking [5–7]. Thus, it is beneficial to obtain low-depth realizations of arbitrary Clifford operations.

Here we provide an explicit algorithm that decomposes arbitrary Clifford operations into a quantum circuit that utilizes single-qubit rotations and, at most, six multiqubit programmable all-to-all entangling gates, which is to the best of our knowledge a factor of 3 better than the state of the art [8]. Previous works have shown implementations of Clifford operations using such multiqubit gates with a gate count that is linear (in the number of qubit) [9, 10], logarithmic [11] or constant [8, 12], with Ref. [12] greatly inspiring this work.

Explicitly, we consider multiqubit Clifford gates over n qubits of the form,

$$U_{\text{MQ}}^{(P)}(\xi) = e^{-i\frac{\pi}{2}\sum_{k=1}^{n} \xi_{kk} P_k - i\frac{\pi}{4}\sum_{k>j}^{n} \xi_{kj} P_k P_j}, \qquad (1)$$

where P_k is the $P \in \{X,Y,Z\}$ Pauli operator, acting on the kth qubit and $\xi \in \mathbb{F}_2^{n \times n}$ is an arbitrary symmetric matrix of zeros and ones, such that for $k \neq j$, $\frac{\pi}{4}\xi_{kj}$ is a correlated $P \otimes P$ rotation between the kth and jth qubits. We note that $U_{\mathrm{MQ}}^{(\mathbf{Z})}$ is equivalent, up to single-qubit Z rotations, to a layer of arbitrary Control-Z (CZ) gates. Similarly, $U_{\mathrm{MQ}}^{(\mathbf{X})}$, generates correlated $X \otimes X$ rotations and is equivalent up to single-qubit Hadamard gates to $U_{\mathrm{MQ}}^{(\mathbf{Z})}$.

Gates of the form of Eq. (1) arise naturally in trapped ions based quantum computers [13-18], where the long-range Coulomb coupling between the ions underpins the all-to-all programmability [19-25]. We remark that additional quantum computing modalities have the potential to generate such programmable multiqubit interactions [26-29], and can as well benefit from our method.

Similarly to Refs. [12, 30], we consider a decomposition of arbitrary Clifford operations to the form,

$$U_{\rm C} = -L - CX - CZ - L - CZ - L - (2)$$

with -L- a layer of single qubit gates, -CX- a linear reversible circuit and -CZ- a layer of Control-Z gates. With this decomposition clearly two multiqubit gates are used for the two -CZ- layers, thus we focus on showing that the -CX- layer can be implemented with at most five entangling multiqubit gates. Furthermore will show that one of the implementations of the -CX- part ends with a -CZ- layer that can be merged with the following -CZ- layer of Eq. (3). Hence, the Clifford circuit is realized with at most six entangling multiqubit gates, compared to a lower bound of four multiqubit gates [8].

The linear reversible layer, -CX-, over n qubits is represented by an invertible matrix, $M \in \mathbb{F}_2^{n \times n}$, such that the layer operates on a state in the computational basis as $|\boldsymbol{v}\rangle \mapsto |M\boldsymbol{v}\rangle$ (with addition performed modulo 2). Such an operation can be represented efficiently by a sequence of CNOT gate, e.g. by performing Gauss elimination of M, a circuit representing the layer can be formed with at most n^2 CNOTs. Moreover, methods to reduce this depth to $\mathcal{O}\left(n^2/\log\left(n\right)\right)$ are known in the literature [31, 32]. We assume such a CNOT circuit representing -CX- is known (regardless of its depth or the way it is constructed).

Specifically, we make use of the symplectic form formalism, which we briefly recap. The symplectic form formalism provides an efficient representation of Clifford circuits, where each Clifford operator is mapped to a binary matrix acting on a vector space over the finite two-element field, $\mathbb{F}_2 = \{0,1\}$ [33, 34]. Pauli vectors on n qubits (also known as Pauli strings) are represented as binary vectors in \mathbb{F}_2^{2n} , defined by,

$$(X_1^{a_1}Z_1^{b_1}) \otimes \cdots \otimes (X_n^{a_n}Z_n^{b_n}) \mapsto (a_1, \dots, a_n \mid b_1, \dots, b_n),$$
(3)

where each pair (a_i, b_i) specifies whether X_i, Z_i , or Y_i acts on qubit i. Thus, the binary vector $(a \mid b)$ with $a, b \in \mathbb{F}_2^n$ encodes an n-qubit Pauli operator. A Clifford operator then acts linearly on these vectors via a symplectic matrix $S \in GL(2n, \mathbb{F}_2)$ representation, giving a group homomorphism from the Clifford group in $SU(2^n)$ to the symplectic group $Sp(2n, \mathbb{F}_2) \in \mathbb{F}_2^{2n \times 2n}$. Importantly, up to an additional layer of single-qubit Pauli operators, Clifford operators admit a unique characterization through their symplectic matrix representation [35].

Pauli operators either commute or anti-commute. This

^{*} yotam.shapira@quantum-art.tech

is represented in their vector form by the matrix,

$$\Omega = \begin{bmatrix} 0 & -I_n \\ I_n & 0 \end{bmatrix},\tag{4}$$

with I_n the $n \times n$ identity operator, such that two Pauli vectors $u, v \in \mathbb{F}_2^{2n}$ commute (anti-commute) if $u^T \Omega v = 0$ ($u^T \Omega v = 1$) [36]. Clifford operators must preserve these commutation relations, yielding the condition,

$$S^T \Omega S = \Omega. (5)$$

This ensures that the symplectic action faithfully captures the defining property of Clifford gates, i.e. mapping Pauli operators to Pauli operators while preserving commutation.

Let $E_{i,j}$ denote the $n \times n$ elementary matrix with a 1 in position (i,j) and 0 in all other entries. When $i \neq j$, the two-qubit gates $R_{Z_iZ_j}^{1/2} = e^{-i\frac{\pi}{4}Z_iZ_j}$ and $R_{X_iX_j}^{1/2} = e^{-i\frac{\pi}{4}X_iX_j}$ are represented by,

$$S(R_{Z_{i}Z_{j}}^{1/2}) = \begin{bmatrix} I_{n} & 0 \\ E_{i,j} + E_{j,i} & I_{n} \end{bmatrix}, \ S(R_{X_{i}X_{j}}^{1/2}) = \begin{bmatrix} I_{n} & E_{i,j} + E_{j,i} \\ 0 & I_{n} \end{bmatrix},$$
(6)

respectively and for i=j we have $R_{Z_i}^{1/2}=e^{-i\frac{\pi}{4}Z_i}$ and $R_{X_i}^{1/2}=e^{-i\frac{\pi}{4}X_i}$, represented by,

$$S(R_{Z_i}^{1/2}) = \begin{bmatrix} I_n & 0 \\ E_{i,i} & I_n \end{bmatrix}, \quad S(R_{X_i}^{1/2}) = \begin{bmatrix} I_n & E_{i,i} \\ 0 & I_n \end{bmatrix}. \tag{7}$$

Using the definition of $U_{\text{MQ}}^{(Z)}$ and $U_{\text{MQ}}^{(X)}$ above and Eqs. (6,7), we note that for symmetric $\xi \in \mathbb{F}_2^{n \times n}$ i.e., $\xi_{n,m} = \xi_{m,n} \in \{0,1\}$, the multiqubit gate takes the form of a GCZ gate [12]. With this $U_{\text{MQ}}^{(Z)}(\xi)$ and $U_{\text{MQ}}^{(X)}(\xi)$ are represented by,

$$S(U_{\text{MQ}}^{(\text{Z})}(\xi)) = \begin{bmatrix} I_n & 0\\ \xi & I_n \end{bmatrix}, \quad S(U_{\text{MQ}}^{(\text{X})}(\xi)) = \begin{bmatrix} I_n & \xi\\ 0 & I_n \end{bmatrix}, \quad (8)$$

respectively.

Similarly, a CNOT gate with control qubit i and target qubit j is represented by the symplectic matrix,

$$S_{\text{CNOT}_{i \to j}} = \begin{bmatrix} I_n + E_{j,i} & 0\\ 0 & I_n + E_{i,j} \end{bmatrix}.$$
 (9)

Generalizing on this, the circuit representation of linear reversible, -CX-, layer takes the form,

$$S_{\rm CX} = \begin{bmatrix} A & 0 \\ 0 & B \end{bmatrix},\tag{10}$$

with $A, B \in \mathbb{F}_2^{n \times n}$ invertible matrices (due to the block form and the fact that S is invertible). Furthermore, utilizing the symplectic condition in Eq. (5) and applying it on the block-diagonal symplectic form of Eq. (10), we obtain,

$$S_{\mathrm{CX}}^{T} \Omega S_{\mathrm{CX}} = \Omega. \tag{11}$$

Recalling that $I_n = -I_n$ in \mathbb{F}_2 we conclude that,

$$B^T A = A^T B = I_n, (12)$$

so that A and B^T are reciprocals.

Next, we decompose $B = S_1S_2$, with S_k being symmetric matrices. Such a decomposition exists and is found efficiently [37]. With these identities and this decomposition we note that S_{CX} is precisely formed by (see step-by-step realization in the SM [38]),

$$S(CX) = S\left(U_{MQ}^{(X)}\left(S_{2}^{-1}\right)\right) S\left(U_{MQ}^{(Z)}\left(S_{2}\right)\right) S\left(U_{MQ}^{(X)}\left(S_{2}^{-1}+S_{1}\right)\right) S\left(U_{MQ}^{(Z)}\left(S_{1}^{-1}\right)\right) S\left(U_{MQ}^{(X)}\left(S_{1}\right)\right),$$

$$(13)$$

or alternatively,

$$S(CX) = S\left(U_{MQ}^{(Z)}\left(S_{2}\right)\right) S\left(U_{MQ}^{(X)}\left(S_{2}^{-1}\right)\right) S\left(U_{MQ}^{(Z)}\left(S_{2}+S_{1}^{-1}\right)\right)$$

$$S\left(U_{MQ}^{(X)}\left(S_{1}\right)\right) S\left(U_{MQ}^{(Z)}\left(S_{1}^{-1}\right)\right). \tag{14}$$

Finally, since the symplectic matrix determines the Clifford operator up to a layer of single qubit Pauli rotations, we conclude that the expression for the -CX- layer comprises at most 5 entangling multiqubit gates and is given by,

$$CX = U_{MQ}^{(X)}(S_2) U_{MQ}^{(Z)}(S_2^{-1}) U_{MQ}^{(X)}(S_1 + S_2^{-1}) U_{MO}^{(Z)}(S_1^{-1}) U_{MQ}^{(X)}(S_1) e^{i\frac{\pi}{2}\sum_k \mu_k Z_k} e^{i\frac{\pi}{2}\sum_k \eta_k X_k},$$
(15)

or alternatively,

$$CX = U_{MQ}^{(Z)} (S_2^{-1}) U_{MQ}^{(X)} (S_2) U_{MQ}^{(Z)} (S_1^{-1} + S_2) U_{MQ}^{(X)} (S_1) U_{MQ}^{(Z)} (S_1^{-1}) e^{i\frac{\pi}{2} \sum_k \tilde{\mu}_k Z_k} e^{i\frac{\pi}{2} \sum_k \tilde{\eta}_k X_k},$$
(16)

where the coefficients μ_k , η_k , $\tilde{\mu}_k$, $\tilde{\eta}_k \in \{0,1\}$ are determined by the symplectic phase vector associated with the -CX- layer and the gates on the right hand-side of Eq. (15) and Eq. (16).

Crucially, the latter decomposition, in Eq. (15), terminates with a $U_{\rm MQ}^{({\rm Z})}$ gate, and can therefore be merged with the following $-{\rm CZ}-$ layer, further reducing the multiqubit gate count.

We note that in the case that B from Eq. (10) is symmetric then the decomposition $B = S_1S_2$ is trivially satisfied with $S_1 = I$, resulting in at most three multiqubit gates in Eqs. (15) and (16).

Next, we investigate the drive power necessary for the implementation of our decomposition. The drive power is an important quantity as many fundamental gate-errors naturally scale with the drive power, e.g. unwanted photon scattering. For trapped-ions qubits, it has been

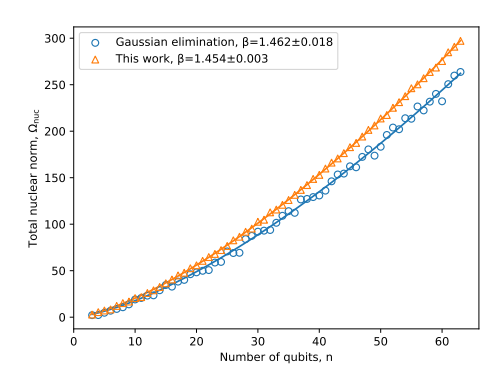


FIG. 1: Total nuclear norm of an implementation using a standard Gaussian elimination to $\sim n^2$ two-qubit gate followed by a merge of parallel operations (blue circles), compared to the total nuclear norm of the constant-cost implementation of this work (orange triangles), showing that the depth reduction is performed with comparable resources. We fit this data to a power law (solid), showing that the total nuclear norm scales approximately as $\sim n^{3/2}$ for both methods.

shown that the gate drive power scales as $\operatorname{nuc}(\xi)$, the nuclear-norm of ξ , i.e. the L_1 norm of its eigenvalues [21]. To investigate this aspect of our decomposition we generate random linear reversible layers, M, and construct their corresponding CNOT circuit with Gaussian elimination. We then decompose them according to Eqs. (13) and (14).

There are many degrees of freedom in the decomposi-

tion of B to a product of two symmetric matrices. These are utilized in order to reduce, in a graph walker method, the resulting total nuclear norm of the decomposition, $\Omega_{\rm nuc}$. Addition reduction is obtained by virtual qubit permutations, as done in Refs. [18, 39].

Figure 1 shows the total nuclear norm of the decomposition, $\Omega_{\rm nuc}$, of random instances of $-{\rm CX}-$ (orange triangles) for varying number of qubits between 3 and 63 (horizontal). This is compared to the total nuclear norm used by a standard decomposition based on the Gaussian elimination, i.e. obtained by implementing CNOT gates with two-qubit $Z \otimes Z$ gates and single-qubit gates and merging parallel operations to MQ gates (blue circles). As seen, our constant-cost implementation has a similar total nuclear norm to that of the naive implementation. We fit these results to a power law (solid), $\Omega_{\rm nuc} \propto n^{\beta}$, with the results appearing in the legend, showing a consistent scaling within fit error of less than $n^{3/2}$ for both methods.

In conclusions, we have shown a computationally efficient algorithm that implements Clifford operation at a constant-cost of 6 multiqubit gates, based on an implementation of linear reversible, CNOT, circuits with 5 multiqubit gates. We have further investigated the drive power associated with this implementation, showing that it can be achieved with the same resources as standard Gaussian elimination methods, that is, depth and execution times are reduced without incurring additional power.

Beyond immediate applications of these decomposition, we note that it can work in conjunction with generic compilation techniques, where the circuit to be compiled can be 'cut' to blocks separated by Clifford operations, that are then realized with a constant-cost.

- [1] Ewout van den Berg and Kristan Temme. Circuit optimization of hamiltonian simulation by simultaneous diagonalization of pauli clusters. *Quantum*, 4:322, September 2020.
- [2] J. Haferkamp, F. Montealegre-Mora, M. Heinrich, J. Eisert, D. Gross, and I. Roth. Efficient unitary designs with a system-size independent number of non-clifford gates. Communications in Mathematical Physics, 397(3):995–1041, Feb 2023.
- [3] Richard Kueng and David Gross. Qubit stabilizer states are complex projective 3-designs, 2015.
- [4] Huangjun Zhu. Multiqubit clifford groups are unitary 3-designs. *Phys. Rev. A*, 96:062336, Dec 2017.
- [5] Andreas Elben, Steven T. Flammia, Hsin-Yuan Huang, Richard Kueng, John Preskill, Benoît Vermersch, and Peter Zoller. The randomized measurement toolbox. Nature Reviews Physics, 5(1):9–24, Jan 2023.
- [6] Hsin-Yuan Huang, Steven T. Flammia, and John Preskill. Foundations for learning from noisy quantum experiments, 2022.
- [7] Hsin-Yuan Huang, Richard Kueng, and John Preskill. Predicting many properties of a quantum system from

- very few measurements. Nature Physics, 16(10):1050–1057, Oct 2020.
- [8] Richard Cleve, Zhiqian Ding, and Luke Schaeffer. Improved clifford operations in constant commutative depth, 2025.
- [9] Dmitri Maslov and Yunseong Nam. Use of global interactions in efficient quantum circuit constructions. New Journal of Physics, 20(3):033018, mar 2018.
- [10] John Van de Wetering. Constructing quantum circuits with global gates. New Journal of Physics, 23(4):043015, 2021.
- [11] Dmitri Maslov and Ben Zindorf. Depth optimization of cz, cnot, and clifford circuits. *IEEE Transactions on Quantum Engineering*, 3:1–8, 2022.
- [12] Sergey Bravyi, Dmitri Maslov, and Yunseong Nam. Constant-cost implementations of clifford operations and multiply-controlled gates using global interactions. *Physical Review Letters*, 129(23):230501, 2022.
- [13] Lei Feng, Or Katz, Casey Haack, Mohammad Maghrebi, Alexey V. Gorshkov, Zhexuan Gong, Marko Cetina, and Christopher Monroe. Continuous symmetry breaking in a trapped-ion spin chain. *Nature*, 623:713-717, 2023.

- [14] I. Pogorelov, T. Feldker, Ch. D. Marciniak, L. Postler, G. Jacob, O. Krieglsteiner, V. Podlesnic, M. Meth, V. Negnevitsky, M. Stadler, B. Höfer, C. Wächter, K. Lakhmanskiy, R. Blatt, P. Schindler, and T. Monz. Compact ion-trap quantum computing demonstrator. PRX Quantum, 2:020343, Jun 2021.
- [15] R. Yao, W.-Q. Lian, Y.-K. Wu, G.-X. Wang, B.-W. Li, Q.-X. Mei, B.-X. Qi, L. Yao, Z.-C. Zhou, L. He, and L.-M. Duan. Experimental realization of a multiqubit quantum memory in a 218-ion chain. *Phys. Rev. A*, 106:062617, Dec 2022.
- [16] Shuang Guo, Yu-Kun Wu, Bin Zhang, Meng Gong, Ye Lin, Jun Zhai, Zhi-Wei Shen, Le-Jie Wang, Ya-Nan Yang, and Lu-Ming Duan. A site-resolved two-dimensional quantum simulator with hundreds of trapped ions. *Nature*, 630(8017):613–619, 2024.
- [17] David Schwerdt, Lee Peleg, Yotam Shapira, Nadav Priel, Yanay Florshaim, Avram Gross, Ayelet Zalic, Gadi Afek, Nitzan Akerman, Ady Stern, Amit Ben Kish, and Roee Ozeri. Scalable architecture for trapped-ion quantum computing using rf traps and dynamic optical potentials. Phys. Rev. X, 14:041017, Oct 2024.
- [18] Jonathan Nemirovsky, Maya Chuchem, and Yotam Shapira. Efficient compilation of quantum circuits using multi-qubit gates, 2025.
- [19] Nikodem Grzesiak, Reinhold Blümel, Kenneth Wright, Kristin M. Beck, Neal C. Pisenti, Ming Li, Vandiver Chaplin, Jason M. Amini, Shantanu Debnath, Jwo-Sy Chen, and Yunseong Nam. Efficient arbitrary simultaneously entangling gates on a trapped-ion quantum computer. Nature Communications, 11(1):2963, Jun 2020.
- [20] Yotam Shapira, Ravid Shaniv, Tom Manovitz, Nitzan Akerman, Lee Peleg, Lior Gazit, Roee Ozeri, and Ady Stern. Theory of robust multiqubit nonadiabatic gates for trapped ions. *Phys. Rev. A*, 101:032330, Mar 2020.
- [21] Yotam Shapira, Lee Peleg, David Schwerdt, Jonathan Nemirovsky, Nitzan Akerman, Ady Stern, Amit Ben Kish, and Roee Ozeri. Fast design and scaling of multiqubit gates in large-scale trapped-ion quantum computers, 2023.
- [22] Yao Lu, Shuaining Zhang, Kuan Zhang, Wentao Chen, Yangchao Shen, Jialiang Zhang, Jing-Ning Zhang, and Kihwan Kim. Global entangling gates on arbitrary ion qubits. *Nature*, 572(7769):363–367, Aug 2019.
- [23] Pascal Baßler, Matthias Zipper, Christopher Cedzich, Markus Heinrich, Patrick H. Huber, Michael Johanning, and Martin Kliesch. Synthesis of and compilation with time-optimal multi-qubit gates. Quantum, 7:984, April 2023
- [24] Yao Lu, Wentao Chen, Shuaining Zhang, Kuan Zhang, Jialiang Zhang, Jing-Ning Zhang, and Kihwan Kim. Implementing arbitrary ising models with a trapped-ion quantum processor. *Phys. Rev. Lett.*, 134:050602, Feb 2025.
- [25] Yotam Shapira, Jovan Markov, Nitzan Akerman, Ady Stern, and Roee Ozeri. Programmable quantum simulations on a trapped-ion quantum computer with a global drive. Phys. Rev. Lett., 134:010602, Jan 2025.
- [26] Simon J. Evered, Dolev Bluvstein, Marcin Kalinowski, Sepehr Ebadi, Tom Manovitz, Hengyun Zhou, Sophie H. Li, Alexandra A. Geim, Tout T. Wang, Nishad Maskara, Harry Levine, Giulia Semeghini, Markus Greiner, Vladan Vuletić, and Mikhail D. Lukin. High-fidelity parallel entangling gates on a neutral-atom quantum computer. Na-

- ture, 622(7982):268-272, Oct 2023.
- [27] Jeremy T. Young, Przemyslaw Bienias, Ron Belyansky, Adam M. Kaufman, and Alexey V. Gorshkov. Asymmetric blockade and multiqubit gates via dipole-dipole interactions. *Phys. Rev. Lett.*, 127:120501, Sep 2021.
- [28] Eric S. Cooper, Philipp Kunkel, Avikar Periwal, and Monika Schleier-Smith. Graph states of atomic ensembles engineered by photon-mediated entanglement. Nature Physics, 20(5):770-775, May 2024.
- [29] Yongxin Song, Liberto Beltrán, Ilya Besedin, Michael Kerschbaum, Marek Pechal, Fran çois Swiadek, Christoph Hellings, Dante Colao Zanuz, Alexander Flasby, Jean-Claude Besse, and Andreas Wallraff. Constant-depth fan-out with real-time feedforward on a superconducting quantum processor. Phys. Rev. Appl., 24:024068, Aug 2025.
- [30] Sergey Bravyi and Dmitri Maslov. Hadamard-free circuits expose the structure of the clifford group. *IEEE Transactions on Information Theory*, 67(7):4546–4563, 2021.
- [31] Ketan N Patel, Igor L Markov, and John P Hayes. Optimal synthesis of linear reversible circuits. Quant. Inf. Comp, 8(3), 2008.
- [32] KN Patel, IL Markov, and JP Hayes. Efficient synthesis of linear reversible circuits (2003). arXiv preprint quantph/0302002.
- [33] Daniel Gottesman. Stabilizer codes and quantum error correction. California Institute of Technology, 1997.
- [34] Scott Aaronson and Daniel Gottesman. Improved simulation of stabilizer circuits. *Physical Review A*, 70(5):052328, 2004.
- [35] Timothy Proctor and Kevin Young. A simple asymptotically optimal clifford circuit compilation algorithm. arXiv preprint arXiv:2310.10882, 2023.
- [36] Jeroen Dehaene and Bart De Moor. Clifford group, stabilizer states, and linear and quadratic operations over gf (2). Physical Review A, 68(4):042318, 2003.
- [37] Olga Taussky. The role of symmetric matrices in the study of general matrices. *Linear Algebra and its Applications*, 5(2):147–154, 1972.
- [38] Supplemental material, that include further technical details.
- [39] Charles H Baldwin, Karl Mayer, Natalie C Brown, Ciarán Ryan-Anderson, and David Hayes. Re-examining the quantum volume test: Ideal distributions, compiler optimizations, confidence intervals, and scalable resource estimations. Quantum, 6:707, 2022.

Supplemental material

I. STEP-BY-STEP DERIVATION OF EQ. (13) AND (14)

The symplectic matrix of a general CNOT circuit operating on n qubits has the form,

$$S\left(\prod_{k=1,2,3,\dots,n} CNOT_{i_k \to j_k}\right) = \begin{bmatrix} A & 0\\ 0 & B \end{bmatrix}$$
(17)

with A and B being $n \times n$ matrices over the field \mathbb{F}_2 , satisfying Eq. (12), i.e.,

$$A^T B = B^T A = I. (18)$$

For every $B \in GL(n, \mathbb{F}_2)$ one can always find symmetric matrices $S_1, S_2 \in GL(n, \mathbb{F}_2)$ such that $B = S_2S_1$ [37]. From Eq. (18) we conclude that

$$B^T A = S_1 S_2 A = I. (19)$$

We now perform the following steps,

1. We decompose B to a product of two symmetric matrices $S_1, S_2 \in GL(n, \mathbb{F}_2)$ so that,

$$\begin{bmatrix} A & 0 \\ 0 & B \end{bmatrix} = \begin{bmatrix} A & 0 \\ 0 & S_2 S_1 \end{bmatrix}.$$

2. Since S_2 is invertible we can apply a, $S(U_{\text{MQ}}^{(\mathbf{X})}\left(S_2^{-1}\right)) = \begin{bmatrix} I & S_2^{-1} \\ 0 & I \end{bmatrix}$.

$$S(U_{\mathrm{MQ}}^{(\mathrm{X})}\left(S_{2}^{-1}\right))\begin{bmatrix}A & 0 \\ 0 & S_{2}S_{1}\end{bmatrix} = \begin{bmatrix}A & S_{1} \\ 0 & S_{2}S_{1}\end{bmatrix}.$$

3. We then apply a $S(U_{\text{MQ}}^{(Z)}(S_2))) = \begin{bmatrix} I & 0 \\ S_2 & I \end{bmatrix}$ gate so that with Eq. (19) we obtain,

$$S(U_{\mathrm{MQ}}^{(\mathrm{Z})}\left(S_{2}\right))\begin{bmatrix}A & S_{1}\\ 0 & S_{2}S_{1}\end{bmatrix} = \begin{bmatrix}A & S_{1}\\ S_{2}A & S_{2}S_{1} + S_{2}S_{1}\end{bmatrix} = \begin{bmatrix}A & S_{1}\\ S_{2}A & 0\end{bmatrix} = \begin{bmatrix}A & S_{1}\\ S_{1}^{-1} & 0\end{bmatrix}.$$

4. We then apply a $S(U_{\text{MQ}}^{(\mathbf{X})}\left(S_2^{-1}\right)) = \begin{bmatrix} I & S_2^{-1} \\ 0 & I \end{bmatrix}$ and again with Eq. (19) we obtain,

$$S(U_{\text{MQ}}^{(\text{X})}\left(S_{2}^{-1}\right))\begin{bmatrix}A & S_{1}\\ S_{1}^{-1} & 0\end{bmatrix} = \begin{bmatrix}A + S_{2}^{-1}S_{1}^{-1} & S_{1}\\ S_{1}^{-1} & 0\end{bmatrix} = \begin{bmatrix}A + A & S_{1}\\ S_{1}^{-1} & 0\end{bmatrix} = \begin{bmatrix}0 & S_{1}\\ S_{1}^{-1} & 0\end{bmatrix}.$$

5. We then apply a $S(U_{\text{MQ}}^{(\mathbf{X})}\left(S_{1}\right)))=\begin{bmatrix}I&S_{1}\\0&I\end{bmatrix}$ and obtain,

$$S(U_{\mathrm{MQ}}^{(\mathrm{X})}\left(S_{1}\right))\begin{bmatrix}0 & S_{1}\\ S_{1}^{-1} & 0\end{bmatrix} =\begin{bmatrix}I & S_{1}\\ S_{1}^{-1} & 0\end{bmatrix}.$$

6. And then apply a $S(U_{\text{MQ}}^{(\mathbf{Z})}\left(S_{1}^{-1}\right)) = \begin{bmatrix} I & 0 \\ S_{1}^{-1} & I \end{bmatrix}$ which leads to,

$$S(U_{\text{MQ}}^{(\mathbf{Z})}\left(S_{1}^{-1}\right))\begin{bmatrix} I & S_{1} \\ S_{1}^{-1} & 0 \end{bmatrix} = \begin{bmatrix} I & S_{1} \\ 0 & I \end{bmatrix}.$$

The right-hand side of the last equation is by definition $S\left(U_{\text{MQ}}^{(\mathbf{X})}(S_1)\right)$. Thus we conclude that, if $S(\text{CNOT}) = \begin{bmatrix} A & 0 \\ 0 & B \end{bmatrix} = \begin{bmatrix} A & 0 \\ 0 & S_2S_1 \end{bmatrix}$ then,

 $S\left(U_{\mathrm{MQ}}^{(\mathrm{Z})}\left(S_{1}^{-1}\right)\right)\right)\cdot S\left(U_{\mathrm{MQ}}^{(\mathrm{X})}\left(S_{1}\right)\right)\right)\cdot S\left(U_{\mathrm{MQ}}^{(\mathrm{X})}\left(S_{2}^{-1}\right)\right)\right)\cdot S\left(U_{\mathrm{MQ}}^{(\mathrm{Z})}\left(S_{2}\right)\right)\right)\cdot S\left(U_{\mathrm{MQ}}^{(\mathrm{X})}\left(S_{2}^{-1}\right)\right)\cdot S\left(\mathrm{CNOT}\right)=S\left(U_{\mathrm{MQ}}^{(\mathrm{X})}\left(S_{1}\right)\right)\right)$ and recalling that,

$$S\left(U_{\mathrm{MQ}}^{(\mathrm{X})}\left(S^{\prime}\right)\right)\right)S\left(U_{\mathrm{MQ}}^{(\mathrm{X})}\left(S^{\prime\prime}\right)\right)\right)=S\left(U_{\mathrm{MQ}}^{(\mathrm{X})}\left(S^{\prime}+S^{\prime\prime}\right)\right)$$

and

$$S\left(U_{\mathrm{MQ}}^{(\mathrm{Z})}\left(S^{\prime}\right)\right)\right)S\left(U_{\mathrm{MQ}}^{(\mathrm{Z})}\left(S^{\prime\prime}\right)\right)\right)=S\left(U_{\mathrm{MQ}}^{(\mathrm{Z})}\left(S^{\prime}+S^{\prime\prime}\right)\right)$$

we conclude that,

$$S(\text{CNOT}) = S\left(U_{\text{MQ}}^{(X)}\left(S_{2}^{-1}\right)\right) S\left(U_{\text{MQ}}^{(Z)}\left(S_{2}\right)\right) S\left(U_{\text{MQ}}^{(X)}\left(S_{2}^{-1} + S_{1}\right)\right) S\left(U_{\text{MQ}}^{(Z)}\left(S_{1}^{-1}\right)\right) S\left(U_{\text{MQ}}^{(X)}\left(S_{1}^{-1}\right)\right). \tag{20}$$

Where we used the fact that $S\left(U_{\text{MQ}}^{(\text{Z})}\right)$ is its own inverse under \mathbb{F}_2 , or equivalently that $U_{\text{MQ}}^{(\text{Z})}$ is its own inverse up to single-qubit Pauli operators. This completes the proof of Eq. (13). Eq. (14) is proved in a similar manner by multiplying from the right (instead of from the left) the symplectic matrix

Eq. (14) is proved in a similar manner by multiplying from the right (instead of from the left) the symplectic matrix $S(\text{CNOT}) = \begin{bmatrix} A & 0 \\ 0 & S_2 S_1 \end{bmatrix} = \begin{bmatrix} S_2^{-1} S_1^{-1} & 0 \\ 0 & S_2 S_1 \end{bmatrix}$ with appropriate symplectic matrices. To see this explicitly we perform the following steps:

1. Decomposing B to a product of two symmetric matrices $S_1, S_2 \in GL(n, \mathbb{F}_2)$ so that

$$\begin{bmatrix} A & 0 \\ 0 & B \end{bmatrix} = \begin{bmatrix} A & 0 \\ 0 & S_2 S_1 \end{bmatrix}.$$

2. Since S_2 is invertible we can apply a, $S(U_{\text{MQ}}^{(\mathbf{Z})}\left(S_1^{-1}\right)) = \begin{bmatrix} I & 0 \\ S_1^{-1} & I \end{bmatrix}$ from the right hand-side. So that,

$$\begin{bmatrix} A & 0 \\ 0 & S_2S_1 \end{bmatrix} S(U_{\mathrm{MQ}}^{(\mathbf{Z})}\left(S_1^{-1}\right)) = \begin{bmatrix} A & 0 \\ S_2 & S_2S_1 \end{bmatrix}.$$

3. We then apply a $S(U_{MQ}^{(X)}(S_1))) = \begin{bmatrix} I & S_1 \\ 0 & I \end{bmatrix}$ from the right hand-side so that with Eq. (19) we obtain,

$$\begin{bmatrix} A & 0 \\ S_2 & S_2S_1 \end{bmatrix} S(U_{\text{MQ}}^{(\mathbf{X})}\left(S_1\right)) = \begin{bmatrix} A & AS_1 \\ S_2 & S_2S_1 + S_2S_1 \end{bmatrix} = \begin{bmatrix} A & AS_1 \\ S_2 & 0 \end{bmatrix} = \begin{bmatrix} A & S_2^{-1} \\ S_2 & 0 \end{bmatrix}.$$

4. We then apply a $S(U_{\text{MQ}}^{(\mathbf{Z})}\left(S_{1}^{-1})\right)) = \begin{bmatrix} I & 0 \\ S_{1}^{-1} & I \end{bmatrix}$ from the right side and again with Eq. (19) we obtain,

$$\begin{bmatrix} A & S_2^{-1} \\ S_2 & 0 \end{bmatrix} S(U_{\text{MQ}}^{(\mathbf{Z})} \left(S_1^{-1} \right)) = \begin{bmatrix} A + S_2^{-1} S_1^{-1} & S_2^{-1} \\ S_2 & 0 \end{bmatrix} = \begin{bmatrix} A + A & S_2^{-1} \\ S_2 & 0 \end{bmatrix} = \begin{bmatrix} 0 & S_2^{-1} \\ S_2 & 0 \end{bmatrix}.$$

5. We then apply a $S(U_{\text{MQ}}^{(\text{Z})}\left(S_{2}\right)))=\begin{bmatrix}I&0\\S_{2}&I\end{bmatrix}$ from the right and obtain,

$$\begin{bmatrix} 0 & S_2^{-1} \\ S_2 & 0 \end{bmatrix} S(U_{\mathrm{MQ}}^{(\mathbf{Z})}\left(S_2\right)) = \begin{bmatrix} I & S_2^{-1} \\ S_2 & 0 \end{bmatrix}.$$

6. And then apply a $S(U_{\text{MQ}}^{(X)}(S_2^{-1})) = \begin{bmatrix} I & S_2^{-1} \\ 0 & I \end{bmatrix}$ from the right, which leads to,

$$\begin{bmatrix} I & S_2^{-1} \\ S_2 & 0 \end{bmatrix} S(U_{\text{MQ}}^{(\mathbf{X})} \left(S_2^{-1} \right)) = \begin{bmatrix} I & 0 \\ S_2 & I \end{bmatrix}.$$

The right-hand side of the last equation is by definition $S\left(U_{\text{MQ}}^{(\mathbf{Z})}\left(S_{2}\right)\right)$. Thus we conclude that, if $S(\text{CNOT})=\begin{bmatrix}A&0\\0&B\end{bmatrix}=\begin{bmatrix}A&0\\0&S_{2}S_{1}\end{bmatrix}$ then,

$$\left(\mathrm{CNOT}\right) \cdot S\left(U_{\mathrm{MQ}}^{(\mathrm{Z})}\left(S_{1}^{-1}\right)\right) \cdot S\left(U_{\mathrm{MQ}}^{(\mathrm{X})}\left(S_{1}\right)\right)\right) \cdot S\left(U_{\mathrm{MQ}}^{(\mathrm{Z})}\left(S_{1}^{-1}\right)\right)\right) \cdot S\left(U_{\mathrm{MQ}}^{(\mathrm{Z})}\left(S_{2}\right)\right)\right) \cdot S\left(U_{\mathrm{MQ}}^{(\mathrm{X})}\left(S_{2}^{-1}\right)\right)\right) = S\left(U_{\mathrm{MQ}}^{(\mathrm{Z})}\left(S_{2}\right)\right)\right).$$

So that finally we conclude that,

$$S(\text{CNOT}) = S\left(U_{\text{MQ}}^{(\text{Z})}\left(S_{2}\right)\right) S\left(U_{\text{MQ}}^{(\text{X})}\left(S_{2}^{-1}\right)\right) S\left(U_{\text{MQ}}^{(\text{Z})}\left(S_{2}+S_{1}^{-1}\right)\right) S\left(U_{\text{MQ}}^{(\text{X})}\left(S_{1}\right)\right) S\left(U_{\text{MQ}}^{(\text{Z})}\left(S_{1}^{-1}\right)\right). \tag{21}$$